Electroluminescence and field emission of Mg-doped ZnO tetrapods

2006 Nanotechnology 17 5096

(http://iopscience.iop.org/0957-4484/17/20/009)

INSTITUTE OF PHYSICS PUBLISHING NANOTECHNOLOGY
Nanotechnology **17** (2006) 5096–5100 doi:10.1088/0957-4484/17/20/009

Electroluminescence and field emission of Mg-doped ZnO tetrapods

Hui Pan[1], Yanwu Zhu[1], Han Sun[1], Yuanping Feng[1], Chorng-Haur Sow[1] and Jianyi Lin[1,2]

[1] Department of Physics, National University of Singapore, 2 Science Drive 3, 117542, Singapore
[2] Institute of Chemical and Engineering Sciences, 1 Pesek Road, Jurong Island, 627833, Singapore

Received 19 July 2006, in final form 20 August 2006
Published 22 September 2006
Online at stacks.iop.org/Nano/17/5096

Abstract
ZnO tetrapods doped with Mg (Mg-ZnOTs) were produced by thermally oxidizing Zn and Mg powders. TEM and XRD patterns indicated that Mg-ZnOTs were crystalline with wurtzite structure. The transport measurements of Mg-ZnOT powder demonstrated that Mg-doped ZnO tetrapods are characteristic of a semiconductor with lower threshold voltage. Two peaks were clearly observed in the electroluminescence spectra. The blue light emission is related to the inter-band transition. The green or yellow light emission was induced by impurity centre recombination. Mg-doped ZnO exhibited better field emission properties with higher emission current density and lower turn-on field than pure ZnO nanowires. And ZnO with higher Mg content exhibited better field-emission properties with higher emission current density than ZnO with lower Mg content.

1. Introduction

As a wide band gap (E_g = 3.35 eV) semiconductor with a large exciton binding energy (60 meV), ZnO is of great interest for applications in low-voltage and short-wavelength electro-optical devices, such as light-emitting diodes and diodes lasers [1, 2]. ZnO nanostructures can lower the threshold of optical gain media because of the quantum size effects and the enhancement of radiative carriers' recombination, which have recently been the focus of intensive researches [1–5]. Typically energy-stimulated ZnO [6–11] exhibits strong UV light emissions due to the radiative decay of excitons. But it may also emit a broad visible light, which is most commonly green, if defects exist in the ZnO lattice. Different ZnO nanostructures (such as nanowires and nanobelts) with visible luminescence have been produced using various methods [6–11]. For a better control of the electrical and optical properties of ZnO, the doping effect has attracted researchers' interest. Gallium doping was reported to lower the threshold electrical field in the field-emission measurements [12]. Alloying ZnO with MgO (E_g = 7.8 eV) was shown to enable the control of the band gap [13], and the photoluminescence properties of Mg-doped ZnO thin films depended on the content of Mg in the ZnO [14]. Recently, Mg-doped ZnO nanowires and nanocrystals have been reported [15–17]. Nevertheless there is no study on the electroluminescence and field emission of Mg-doped ZnO nano-tetrapods. In this study, we prepared Mg-doped ZnO nano-tetrapods by oxidative vapour condensation of Zn and Mg powders. Their electroluminescence and field emission were studied for the first time.

2. Experimental details

Mg-doped ZnO nano-tetrapods were produced following the same process as reported in [16]. Briefly, Zn and Mg powders (2:1 in atomic ratio) in an alumina boat were placed at the centre of a quartz tube, which was heated to 800 °C at a rate of 20 °C min^{-1} with a protective helium (He) flow at 100 standard cubic centimetres per minute (sccm). Oxygen (O_2) flow at a speed of 20 sccm was introduced to the furnace after the desired furnace temperature had been reached. The mixed gas, O_2 and He, was maintained throughout the whole reaction process, usually ∼30 min. After the reaction, the sample was cooled down to room temperature in the protective He flow. After taking out the boat, a lot of Mg powder was remained at the centre of the ceramic boat after the reaction, which means that only a little Mg took part in the reaction. Two samples were prepared for comparison. Mg-ZnOT-A was deposited within the alumina boat in the zone close to the centre of

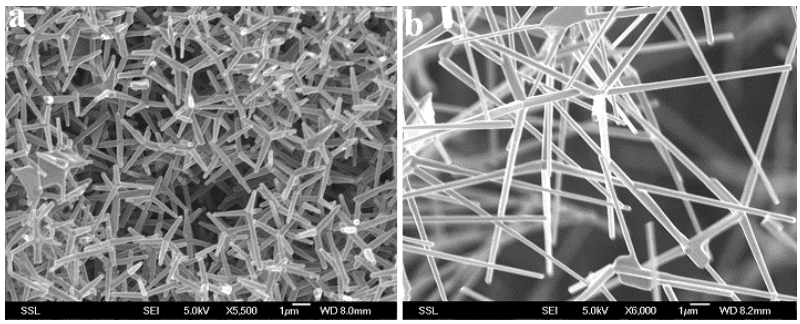

Figure 1. SEM images of (a) Mg-ZnOT-A and (b) Mg-ZnOT-B.

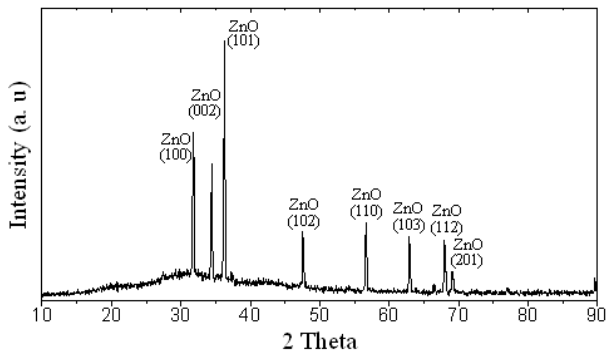

Figure 2. XRD pattern of the Mg-doped ZnO nano-tetrapods.

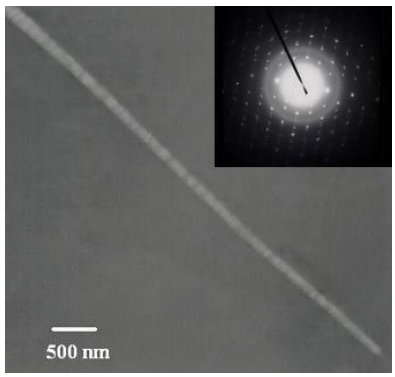

Figure 3. TEM image and selected-area electron diffraction pattern of Mg-ZnOT-A.

the reaction tube (around 800 °C) whereas Mg-ZnOT-B was collected from the zone close to the gas outlet (around 200 °C).

The as-grown Mg-ZnOT-A and Mg-ZnOT-B were characterized by scanning electron microscope (SEM, JEOL JSM-6700F), high-resolution transmission electron microscope (HRTEM, JEOL 2010 at 200 kV), XRD (Brucker AXS D8) and an x-ray photoelectron spectroscope (XPS, ESCA Lab II).

The measurements of field emission (FE) of the samples were carried out in a two-parallel-plate set-up with a high vacuum of about 5×10^{-7} Torr [18]. The powder sample was attached to a Cu substrate, which serves as cathode, by using double-sided copper tape. Indium tin oxide (ITO) glass covered with a layer of phosphor was employed as the anode. A polymer film was used as a spacer and the distance between the electrodes was kept at 100 μm. A Keithley 237 high-voltage source measurement unit (SMU) was used to apply a voltage from 0 to 600 V and to measure the emission current. All the measurements were performed at room temperature. The electron transportation property was studied using the same equipment (SMU), but without the spacer. Electroluminescence (EL) was recorded by a fibre light detector (Ocean Optics).

3. Results and discussions

Figure 1 shows the SEM images of the two samples. Mg-ZnOT-A in figure 1(a) is tetrapods with diameter ranging from 100 to 300 nm and length in the range 3–4 μm. Mg-ZnOT-B, which was produced outside the alumina boat, has smaller diameters (about 80 nm) and a larger length up to 10 μm (figure 1(b)) due to insufficient Zn vapour.

The XRD diffraction pattern in figure 2 indicates that both Mg-ZnOT-A and -B have the wurtzite structure. No appearance of the MgO peaks in the XRD pattern reveals that the content (x) of Mg in the Mg-doped ZnO nano-tetrapods is less than 0.1 [15], and Mg doping did not change the wurtzite structure of ZnO because of its small content. The selected-area electron diffraction (SAED) pattern taking from one isolated Mg-doped ZnO nano-tetrapod (see figure 3) shows that the Mg-ZnOT is basically single crystal with some polycrystalline mixture. The XPS spectrum of Mg-ZnOT-A (see figure 4) confirms the existence of Mg. The Mg content in Mg-ZnOT-A is higher than that in Mg-ZnOT-B as indicated by higher intensity ratio of Mg2p/Zn2p$^{3/2}$ (0.003 16 for Mg-ZnOT-A and 0.000 98 for Mg-ZnOT-B) in figure 4, which is further confirmed by following electron transport measurement.

Figure 5 shows the results of electron transport measurement of the two samples. There exists a threshold voltage in the I–V curve, below which no current can be detected. This is characteristic of semiconductors. The value is lower for Mg-ZnOT-A (1.0 V in figure 5(a)) than for Mg-ZnOT-B (1.3 V in figure 5(b)). The current density of Mg-ZnOT-A is much larger than that of Mg-ZnOT-B under the same voltage. This appears to result from higher Mg concentration in Mg-ZnOT-A because higher doping leads to higher electron concentration, which is consistent with the XPS study. Two peaks are observable in the electroluminescence (EL) spectra in figure 6. For Mg-ZnOT-A, the EL peak centred at 620 nm, which is related to the yellow emission, is rather broad and strong, while the peak at 379 nm, corresponding

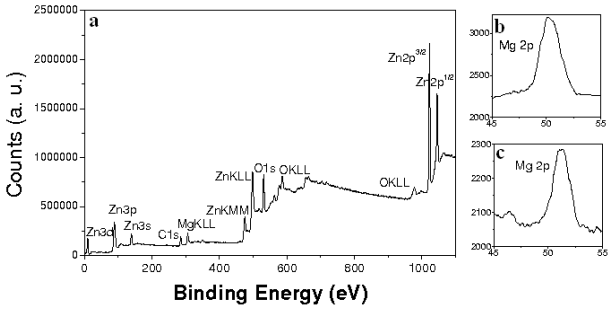

Figure 4. (a) The XPS survey spectrum of Mg-doped ZnO nano-tetrapods, (b) Mg 2p core level spectrum of Mg-ZnOT-A and (c) Mg 2p core level spectrum of Mg-ZnOT-B.

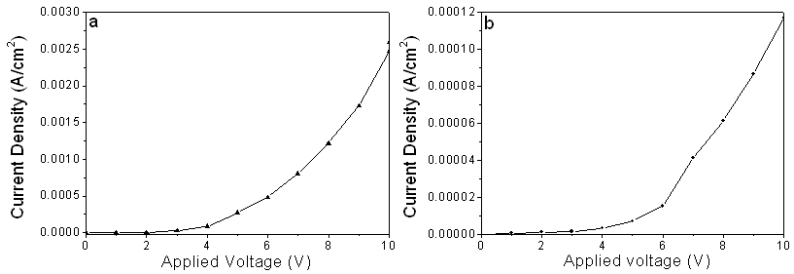

Figure 5. Electron transport I–V curves for (a) Mg-ZnOT-A and (b) Mg-ZnOT-B.

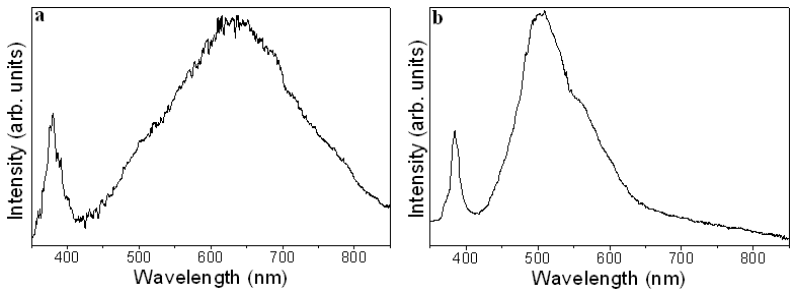

Figure 6. Electroluminescence spectra for (a) Mg-ZnOT-A and (b) Mg-ZnOT-B.

to blue emission, is of low intensity (figure 6(a)). For Mg-ZnOT-B, in addition to the low-intensity peak at 384 nm, a pronounced peak is located between 450 and 550 nm, which is related to green emission (figure 6(b)).

A p–n junction operated under forward bias has been used to illustrate injection electroluminescence [19]. Under forward bias, majority carriers from both sides of the junction cross the internal potential barrier and enter the material at the other side where they are the minority type of carrier and cause the local minority carrier population to be larger than normal. The excess minority carriers diffuse away from the junction, recombining with majority carriers, which leads to the emission of photons. The injected electron under the applied DC field takes part in a radiative recombination with holes and hence gives rise to an emitted photon. The radiative recombination processes include inter-band transitions and impurity centre recombination. The inter-band transition corresponds to the peak around 380 nm (3.27 eV), which is related to and slightly less than the band gap due to the thermal excitation. The band gap of ZnO increases with the increase of the concentration of the Mg substitution, which leads to the larger inter-band transition energy in sample A (3.29 eV) compared with sample B (3.26 eV). The impurity centre recombination (such as interstitial Mg) is responsible for the light emission with wavelength above 450 nm. The lower threshold voltage and higher current of Mg-ZnOT-A (figure 5(a)) indicate that the concentration of the Mg dopant in Mg-ZnOT-A is much larger than that in Mg-ZnOT-B. The impurity centres within the band gap can trap electrons and holes, which lead to electron–hole recombination and emission of photons. The higher the impurity concentration, the wider the impurity band in the forbidden band. The required energy to excite electrons from the valence band to the impurity level is reduced. This fact is responsible for the yellow light emission (620 nm) of Mg-ZnOT-A and for the green light emission (510 nm) of Mg-ZnOT-B. This means that the energy band gap structure of ZnO can be adjusted by changing the Mg doping level.

The field-emission current density as a function of the macroscopic electric field is shown in figure 7 for the

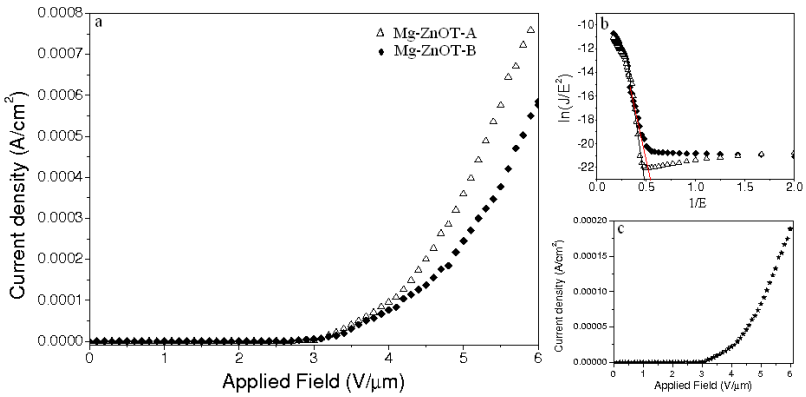

Figure 7. (a) Field-emission I–V curves of Mg-ZnOTs, (b) FN plots of Mg-ZnOTs, and (c) field emission of the undoped ZnO nanostructures.

Mg-doped ZnO nano-tetrapods. The turn-on fields are 2.6 V μm^{-1} for Mg-ZnOT-A and 2.8 V μm^{-1} for Mg-ZnOT-B (see figure 7(a)). The emission current densities reach 0.76 mA cm^{-2} for Mg-ZnOT-A and 0.58 mA cm^{-2} for Mg-ZnOT-B at 6.0 V μm^{-1}. The Fowler–Nordheim (FN) plots for the measured samples are shown in figure 7(b). It is clear that the measured data fit well with the FN equation [20]:

$$\ln\left(\frac{J}{E^2}\right) = \ln\left(\frac{A\beta^2}{\varphi}\right) - \frac{B\varphi^{3/2}}{\beta E} \qquad (1)$$

where J is the emission current density (A cm^{-2}), E is the applied field (V μm^{-1}), $A = 1.543 \times 10^{-6}$ A eV V^{-2}, $B = 6.833 \times 10^3$ $eV^{-3/2}$ V μm^{-1}, β is the field enhancement factor, and φ is the work function of emitter material (5.3 eV for ZnO [21]). The calculated field enhancement factor β from the slope of figure 7(b) (as indicated by the lines) is 2327 for Mg-ZnOT-A and 1690 for Mg-ZnOT-B, respectively. The β-value is related to the geometry, crystal structure, conductivity, work function, and nanostructure density. Figure 7(c) shows the field emission of pure ZnO nanostructures. It is clear that the field-emission property of Mg-doped ZnO nanostructures is better than that of the undoped samples. The field-emission current density of the Mg-ZnOT is better than or at least comparable with those reported in the literature for well-aligned ZnO nanofibres [20] and pure ZnO tetrapods [22]. And the field-emission property of Mg-doped ZnO nano-tetrapods is comparable with that of Ga-doped ZnO nanorods [14] and needle-like ZnO nanorod arrays [23], although our samples were randomly oriented. The Mg doping may enhance the conductivity of ZnO as indicated in the I–V curves (figure 5), which leads to the better field-emission property of Mg-doped ZnO nano-tetrapods. The field-emission current density of Mg-ZnOT-A is higher than that of Mg-ZnOT-B, which is attributed to its higher Mg concentration, lower density and lower resistance (figures 4 and 5).

4. Conclusions

In summary, Mg-doped ZnO nano-tetrapods were produced by thermally oxidizing Zn and Mg powders. The radiative inter-band transition and impurity centre recombination were responsible for the light emission observed in the electroluminescence spectra. The blue light emission is related to the inter-band transition. The long-wavelength light emission is induced by impurity centre recombination. The exact peak position is closely related to the Mg concentration. Yellow light emission is observed in Mg-ZnOT-A, and green light emission in Mg-ZnOT-B, because the Mg concentration of sample A is higher than that of sample B, as indicated by the I–V curves. Mg-ZnOT-A exhibits better field-emission properties with higher emission current density than Mg-ZnOT-B due to the higher conductivity induced by the higher Mg concentration. These Mg-doped ZnO nano-tetrapods should be useful in electronic and optical nanodevices.

References

[1] Bagnall D M, Chen Y F, Zhu Z, Yao T, Koyama S, Shen M Y and Goto T 1997 *Appl. Phys. Lett.* **70** 2230
[2] Cao H, Xu J Y, Zhang D Z, Chang S-H, Ho S T, Seelig E W, Liu X and Chang R P H 2000 *Phys. Rev. Lett.* **84** 5584
[3] Wong E M and Searson P C 1999 *Appl. Phys. Lett.* **74** 2939
[4] Jin B J, Bae S H, Lee S Y and Im S 2000 *Mater. Sci. Eng.* B **71** 301
[5] Pieralli C and Hoummady M 1998 *Appl. Phys.* A **66** 377
[6] Wang Z L 2004 *J. Phys.: Condens. Matter* **16** R829
[7] Yu S, Wang C, Yu J, Shi W, Deng R and Zhang H 2006 *Nanotechnology* **17** 3607
[8] Suehiro J, Nakagawa N, Hidaka S, Ueda M, Imasaka K, Higashihata M, Okada T and Hara M 2006 *Nanotechnology* **17** 2567
[9] Djurisic A B, Leung Y H, Choy W C H, Cheah K W and Chan W K 2004 *Appl. Phys. Lett.* **84** 2635
[10] Hsu H, Cheng H, Wu C, Huang H, Lee Y and Hsieh W 2006 *Nanotechnology* **17** 1404
[11] Xu F, Yuan Z, Du G, Ren T, Bouvy C, Halasa M and Su B 2006 *Nanotechnology* **17** 2588
[12] Xu C X, Sun X W and Chen B J 2004 *Appl. Phys. Lett.* **84** 1540
[13] Ohtomo A, Kawasaki M, Koida T, Masubuchi K, Koinuma H, Sakurai Y, Yoshida Y, Yasuda T and Segawa Y 1998 *Appl. Phys. Lett.* **72** 2466
[14] Zhao D, Liu Y, Shen D, Lu Y, Zhang J and Fan X 2001 *J. Appl. Phys.* **90** 5561
[15] Ku C H, Chiang H H and Wu J J 2005 *Chem. Phys. Lett.* **404** 132
[16] Pan H, Luo J, Sun H, Feng Y, Poh C and Lin J 2006 *Nanotechnology* **17** 2963

[17] Bang J, Yang H and Holloway P H 2006 *Nanotechnology* **17** 973
[18] Zhu Y W, Yu T, Cheong F C, Xu X J, Lim C T, Tan V B C, Thong J T L and Sow C H 2005 *Nanotechnology* **16** 88
[19] Fox M 2001 *Optical Properties of Solids* (Oxford: Oxford University Press) p 103
[20] Lee C J, Lee T J, Lyu S C, Zhang Y, Ruh H and Lee H J 2002 *Appl. Phys. Lett.* **81** 3648
[21] Tang C C and Bando Y 2003 *Appl. Phys. Lett.* **83** 659
[22] Li Q H, Wan Q, Chen Y J, Wang T H, Jia H B and Yu D P 2004 *Appl. Phys. Lett.* **85** 636
[23] Zhao Q, Zhang H Z, Zhu Y W, Feng S Q, Sun X C, Xu J and Yu D P 2005 *Appl. Phys. Lett.* **86** 203115